Journal of Oral Science, Vol. 59, No. 3, 329-335, 2017

Original

The expression and significance of the *HOXA7* gene in oral squamous cell carcinoma

Xiaofeng Duan, Hao Chen, Hong Ma, and Yufeng Song

Oral and Maxillofacial Surgery Department, Affiliated Stomatology Hospital, Guizhou Medical University, Guizhou, P. R. China

(Received August 29, 2016; Accepted October 4, 2016)

Abstract: The aim of this study was to examine the expression of *HOXA7* in oral squamous cell carcinoma (OSCC) and its correlation with clinical features. Sixty tissue specimens were collected from 60 OSCC patients who underwent surgical treatment at the Stomatological Hospital affiliated to Guizhou Medical University. Sixty specimens of normal oral tissue were also collected from 60 age- and sex-matched healthy controls. Expression of *HOXA7* was assessed by real time polymerase chain reaction and immunohistochemistry. Relative to the control group, *HOXA7* was up-regulated in OSCC tissues at both the mRNA and protein levels ($P < 0.05$), and *HOXA7* expression in poorly differentiated cancers was higher than that in highly differentiated cancers ($P < 0.05$). *HOXA7* expression was higher in patients with stage III and IV cancer than in patients with stage I and II cancer ($P < 0.05$). Higher *HOXA7* expression was also associated with the presence of vascular and nerve invasion, and lymph node and distant metastasis. *HOXA7* expression in OSCC is markedly increased at both the mRNA and protein levels, and this is positively correlated with clinical stage and the degree of tumor differentiation. These data suggest that *HOXA7* could serve as a diagnostic marker for OSCC or a treatment target.

Correspondence to Dr. Yufeng Song, Oral and Maxillofacial Surgery Department, Affiliated Stomatology Hospital, Guizhou Medical University, No. 28, Guiyi Road, Guizhou 550004, P. R. China
Fax: +86-8516855119 E-mail: songyufeng0625@163.com

J-STAGE Advance Publication: May 19, 2017
Color figures can be viewed in the online issue at J-STAGE.
doi.org/10.2334/josnusd.16-0634
DN/JST.JSTAGE/josnusd/16-0634

Keywords: oral squamous cell carcinoma; *HOXA7*; clinical features.

Introduction

Oral cancer ranks eighth in terms of total cancer incidence worldwide, and is the third most common type of malignancy in South-central Asia (1). Oral squamous cell carcinoma (OSCC) accounts for more than 80% of all malignant oral and maxillofacial tumors. According to the latest data, mortality due to oral carcinoma accounts for 0.88% of all cancer deaths in China (2,3). In the United States, 2-4% of annually diagnosed malignancies are OSCC, resulting in 8,000 deaths each year (4). In addition, OSCC severely affects the life quality of patients, as they suffer difficulty in daily activities such as feeding, communication and other social activities (5).

Multiple genes are involved in tumorigenesis (6). These genes play prominent roles in cell proliferation, differentiation and genome stability (7). *HOXA7* is one of these genes, and plays important roles in cell differentiation and cell morphological development. *HOXA7* is a member of the homologous homeobox gene family located in the HOXA gene cluster on chromosome 7p15-p14, and a recent investigation has suggested that *HOXA7* has critical roles in normal cell proliferation and differentiation during development, while its overexpression can cause malignant tumors (8).

Expression of *HOXA7* has been found to increase markedly in breast cancer (9), ovarian cancer (10), gastric cancer (11), lung cancer (12) and other cancers (13). However, no reports have documented the expression of *HOXA7* in oral neoplasms. In the present study, we examined the expression of *HOXA7* in OSCC tissue using real time-qPCR and immunohistochemistry. We

also evaluated the differences of *HOXA7* expression between OSCC and normal tissue, as well as the correlation between its expression and clinical features.

Materials and Methods

Patients and clinical data

From September, 2013 to December, 2014, 60 OSCC patients who underwent surgery at the Stomatological Hospital affiliated to Guizhou Medical University, China were enrolled in this study. Sixty tissue specimens, one from each patient, were collected, including specimens of tongue, gingiva and mouth floor carcinoma. Patient age, sex, and clinicopathological data were also collected (Table 1). Sixty samples of normal tissue including oral mucosa, gingiva, vermilion and soft palate, were also collected from 60 age- and sex-matched controls during dental visits. All of the OSCC patients underwent surgery and received no other treatments such as chemotherapy, radiation therapy or immunotherapy before or after the surgical procedures. Diagnosis was based on histological tests and confirmed by pathological examination. Patients with heart disease, high blood pressure, diabetes, other systemic diseases or genetic anomalies were excluded.

This study was approved by the Research Ethics Committee of Guizhou Medical University (ID 2016-108). Informed consent was obtained from all of the studied patients.

Real-time qPCR

mRNA was extracted using the paramagnetic particle method in accordance with the manufacturer's instructions (Dynabeads mRNA DIRECTTM, ThermoFisher Scientific, Los Angeles, CA, USA). Briefly, segments of tissue of about 1-2 mm^3 were harvested and immediately stored in RNA*Later* reagent (−80°C). The tissue was then transferred to lysis buffer containing proteolysis enzyme K and incubated at 55°C until complete digestion. Subsequently, 40 μL Dynabeads dT25 was added to each sample and mixed at room temperature for 10 min. The samples were then placed on a magnetic rack. Wash Buffer A was added to each tube and the supernatant was removed without disturbing the Dynabeads pellet. The beads were then washed with Buffer B and the supernatant was removed. The samples were then removed from the magnetic rack and 13 μL Tris-HCl was added to the pellet and the Dynabeads were thoroughly resuspended using a pipette tip. Finally, the suspended Dynabeads were heated in a heat block for 2 min at 80°C to elute off the mRNA. The tubes were then placed immediately on a magnetic rack to concentrate the beads. The supernatant (13 μL in Tris-HCl) containing mRNA was then collected and added directly to 7.5 μL cDNA Synthesis Master Mix (Transcriptor First Strand cDNA Synthesis Kit, Roche, Shanghai, China). These samples were then placed in a thermal cycler at 42°C for 30 min, followed by 85°C for 5 min, and 4°C for 5 min. One microliter of the synthesized cDNA was used in the subsequent PCR reaction in a 10-μL reaction volume containing 5 μL SYBR Green (Light Cycler 480 SYBR Green I Master, Roche) and 4.0 μL primers. The PCR reaction was conducted with a CFX connect Real Time System (Bio-Rad, Hercules, CA, USA) under the following reaction conditions, as described previously (14): pre-denaturation for 5 min at 95°C, denaturation for 10 s at 95°C, and annealing for 30 s at 65°C for a total of 64 cycles. Each sample had three replicates. The mean threshold cycle value was analyzed by the relative quantitative method with *POLR2A* as an internal control. The following primers were used: *HOXA7*, forward: 5'-ctggatgcggtcttcagg-3', Reverse: 5'-ggtagcggttgaagtggaac-3'; *POLR2A* (control) forward: 5'-gcaaattcaccaagagagac-3', reverse: 5'-cacgtcgacaggaacatcag-3'.

Immunohistochemistry and quantification

Immunohistochemistry was conducted according to standard procedures as described previously (15). Briefly, tissue samples were harvested, rinsed with saline and fixed in formalin. The tissue samples were then embedded in paraffin and cut into sections 4 μm thick. The sections were stained with hematoxylin-eosin (HE) to confirm the diagnosis. They were then deparaffinized in xylene and rehydrated in a graded alcohol series, followed by immersion in 3.0% hydrogen peroxide for 10 min at room temperature, and blocking in serum (5% goat serum) for 1 h. The sections were then incubated with a monoclonal primary antibody against *HOXA7* (Abcam, Cambridge, MA, USA) at 4°C overnight, incubated with a secondary biotinylated antibody, and then briefly incubated with streptavidin-biotinylated horseradish peroxidase (Abcam).

For scoring of *HOXA7* expression, 10 fields (400×) from each section were randomly selected under a microscope (Olympus, Tokyo, Japan). *HOXA7* positivity, shown as yellow or brown staining in the cytoplasm, was assessed semi-quantitatively. First, cells with positive staining were counted and the ratio of positive cells was calculated and scored as 0 (<10%), 1 (10-30%), or 2 (>30%). The positive cells were then further quantified by staining intensity as score 0 (weak or no staining), 1 (light yellow staining), or 2 (brownish yellow staining). The two scores were then added together, and a total score of 0-1 was considered as negative (−), 2-3 as posi-

Table 1 *HOXA7* expression in OSCC by IHC and its relationship with clinical and pathological parameters

Variables		*n*	Negative	Positive	Positive rate	*Z*	*P*
Sex	Male	44	8	36	81.8%	−0.576	0.156
	Female	16	2	14	87.5%		
Age	>45	36	8	28	77.8%	−1.837	0.031*
	<45	24	8	16	66.7%		
Tumor size	>2 cm	23	4	19	82.6%	−1.563	0.024*
	<2 cm	37	13	24	64.9%		
Tumor differentiation	I	44	10	34	77.3%	−1.954	0.013*
	II	16	0	16	100%		
Vascular invasion	Y	40	7	33	82.5%	−0.893	0.026*
	N	20	6	14	70.0%		
Nerve invasion	Y	48	7	41	85.4%	−1.262	0.002*
	N	12	3	9	75.0%		
Lymph node metastasis	Y	22	2	20	90.9%	−0.756	0.032*
	N	38	8	30	78.9%		
Distant metastasis	Y	6	1	5	83.3%	−1.235	0.042*
	N	54	9	45	83.3%		

*$P < 0.05$.

tive (+), and 4 as strongly positive (++).

Optical density (OD) analysis was based on photographs of 10 fields (200×, 768 × 556 pixels) from each slide. Mean integrated optical density (MOD) was analyzed using Image pro-plus (Media Cybernetics, Inc., Rockville, MD, USA). MOD was calculated as: MOD = IOD / area (sum), area (sum) being the total area with positive staining.

Statistical analysis

Statistical analyses were conducted using the SPSS statistical software package, version 10.0 (IBM, New York, NY, USA). Chi-squared analysis was used for comparisons between two groups. Student's *t*-test was used for comparisons among multiple groups. Differences at $P < 0.05$ were considered statistically significant.

Results

Normal oral mucosa tissue showed obvious stratification into the cutinized layer, the granular layer, the stratum spinosum and the basal layer (Fig. 1). The cutinized layer is located in the keratinized epithelium, including several layers of hyperkeratosis or parakeratosis of flat cells, staining red with HE. The granular layer is located in the deep surface of the cornified layer, composed of 2-3 layers of cells and characterized by large and flat cells with condensed nuclei. The highly differentiated OSCC tissue showed obvious cancer nests and keratinization beads, whereas OSCC with intermediate differentiation showed obvious cancer nests, but not beads. Poorly differentiated OSCC did not show cancer nests and keratinization beads.

HOXA7 expression at the protein level was assessed by IHC in 60 samples of OSCC tissue and 60 samples of normal tissue. Increased expression of *HOXA7* protein was observed as yellow or brown staining in the cancer cell cytoplasm (Fig. 2B, C, D), while weak or no staining was observed in normal tissue (Fig. 2A). As shown in Table 2, the proportion of cells with positive *HOXA7* staining (+ or ++) was 70.0% in the cancer and 33.3% in the normal group. The difference was statistically significant by chi-squared analysis ($\chi^2 = 8.07$, $P < 0.01$).

We then analyzed the correlation between positive staining for *HOXA7* in the 60 OSCC tissue samples and clinicopathological parameters. We found that the proportion of individuals with positive *HOXA7* expression was higher (100%) for moderately and poorly differentiated OSCC than for highly differentiated OSCC (77.3%) ($z = -1.954$, $P = 0.013$) (Table 1). Similarly, the number of patients with positive *HOXA7* staining increased significantly with progression of the clinical stage and disease severity, characterized by features such as vascular invasion ($P = 0.026$), nerve invasion ($P = 0.002$), lymph node metastasis ($P = 0.032$) and distal metastasis ($P = 0.042$). Interestingly, *HOXA7* expression was correlated positively with tumor size, and patients with tumors measuring >2 cm showed a higher *HOXA7* level than patients with tumors measuring <2 cm ($P = 0.024$). *HOXA7* expression was also correlated with patient age, those older than 45 yr having a higher ratio of *HOXA7* positivity ($P = 0.031$). However, no correlation between *HOXA7* expression and gender was observed ($P = 0.156$).

To further quantify the staining demonstrated by IHC, we measured the MOD value of *HOXA7* in OSCC and normal tissues (Table 3). We found that the MOD value

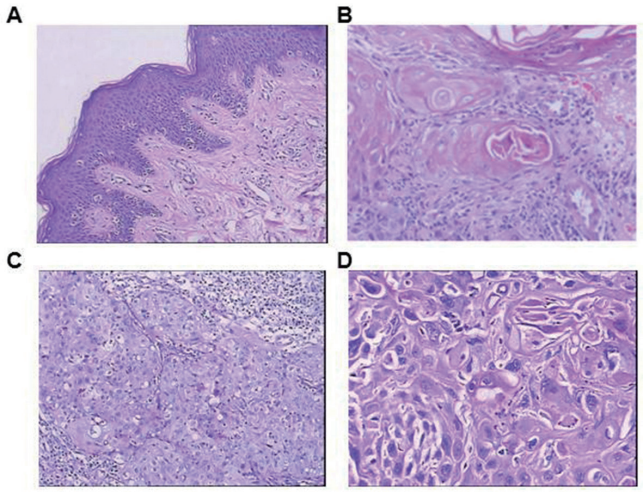

Fig. 1 Representative images of HE staining of normal oral mucosa tissue (A), highly differentiated OSCC (B), moderately differentiated OSCC (C) and poorly differentiated OSCC (D) (200×).

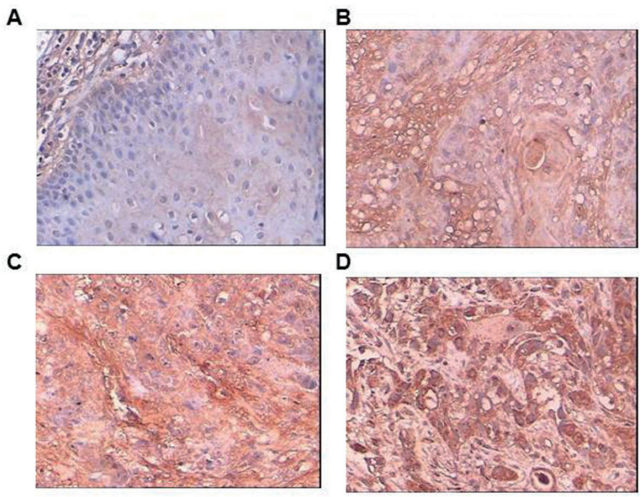

Fig. 2 Representative images of immunohistochemical (IHC) staining of normal oral mucosa tissue (A), highly differentiated OSCC (B), moderately differentiated OSCC (C) and poorly differentiated OSCC (D) (200×).

Table 2 *HOXA7* staining in OSCC and normal tissue by IHC

Groups	*HOXA7* expression					χ^2	*P*
	n	−	+	++	Positive rate (%)		
Normal	60	40	16	4	33.3	8.07	<0.01
OSCC	60	18	30	12	70.0		

Table 3 Expression of *HOXA7* in OSCC and normal tissue by optical density analysis

Groups	Cases (*n*)	MOD (X ± S)	*t*	*P*
Normal	60	0.051 ± 0.015	−24.049	<0.001
OSCC	60	0.448 ± 0.127		

MOD: Mean integrated optical density.

for *HOXA7* in OSCC was higher than that in normal tissue, as demonstrated by two independent samples *t*-test ($t = -24.049$, $P < 0.001$). This result was consistent with the earlier counting result. Therefore, we concluded that the expression of *HOXA7* protein in OSCC was higher than that in normal tissues.

We further examined the correlation between the MOD value and clinical and pathological parameters (Table 4). The *HOXA7* MOD value in poorly and moderately differentiated OSCC was higher than that in highly differentiated OSCC (0.43 ± 0.14 vs. 0.50 ± 0.07, $P = 0.007$). The MOD value increased significantly with the increase in tumor size ($P = 0.002$), the presence of vascular invasion ($P = 0.022$) and nerve invasion ($P < 0.001$), lymph node metastasis ($P = 0.047$) and distant metastasis ($P = 0.001$). However, no correlation between *HOXA7* expression and age or gender was observed ($P > 0.05$).

HOXA7 expression was amplified by qRT-PCR with a Ct value between 18 and 35. The specificity of *HOXA7* amplification was further verified by a single-peak melting curve (8). The relative expression of *HOXA7* was 0.038 ± 0.020 in normal tissue and 1.125 ± 0.544 in OSCC tissues, the difference being statistically significant by *t*-test ($t = -15.466$, $P < 0.001$) (Table 5). Thus, *HOXA7* expression was up-regulated in OSCC tissues at both the mRNA and protein levels.

The correlation between *HOXA7* expression at the mRNA level and clinicopathological features was also analyzed (Table 6). Expression of *HOXA7* in moderately and poorly differentiated OSCC was higher than that in highly differentiated OSCC ($P < 0.001$). Similarly, patients with tumors larger than 2 cm had higher *HOXA7* expression than those with tumors measuring < 2 cm ($P < 0.001$). *HOXA7* expression also increased with the presence of vascular invasion ($P = 0.003$) and nerve invasion ($P = 0.004$), lymph node metastasis ($P < 0.001$) and distant metastasis ($P = 0.001$). Finally, no correlation between *HOXA7* mRNA level and age or gender was found ($P > 0.05$).

Discussion

In this study, we found that *HOXA7* expression in OSCC was markedly increased at both the mRNA and protein levels. Moreover, the increased expression of *HOXA7* was correlated positively with clinical stage and tumor

Table 4 Correlation of *HOXA7* expression as measured by optical density with other parameters in OSCC

Variables		*n*	MOD	*t*	*P*
Sex	Male	44	0.45 ± 0.13	0.222	0.825
	Female	16	0.44 ± 0.13		
Age	>45	36	0.42 ± 0.12	−1.941	0.057
	<45	24	0.49 ± 0.14		
Tumor size	>2 cm	37	0.49 ± 0.11	3.232	0.002
	<2 cm	23	0.39 ± 0.12		
Tumor differentiation	I	44	0.43 ± 0.14	−2.825	0.007
	II	16	0.50 ± 0.07		
Vascular invasion	Y	40	0.47 ± 0.12	2.355	0.022
	N	20	0.40 ± 0.13		
Nerve invasion	Y	48	0.48 ± 0.11	5.007	<0.001
	N	12	0.31 ± 0.08		
Lymph node metastasis	Y	22	0.48 ± 0.08	2.033	0.047
	N	38	0.43 ± 0.14		
Distant metastasis	Y	6	0.54 ± 0.05	3.884	0.001
	N	54	0.44 ± 0.13		

Table 5 Relative expression of *HOXA7* at the mRNA level in normal oral tissues and OSCC

Groups	Cases (*n*)	*HOXA7* (X ± S)	*t*	*P*
Normal	60	0.038 ± 0.020	−15.466	<0.001
OSCC	60	1.125 ± 0.544		

Note: Oral squamous cell carcinoma compared to normal tissue. *$P < 0.05$.

Table 6 Correlation between *HOXA7* expression at the mRNA level and the clinical features of OSCC

Variables		*n*	*HOXA7* mRNA	*t*	*P*
Sex	Male	44	1.14 ± 0.56	0.329	0.743
	Female	16	1.09 ± 0.52		
Age	>45	36	1.12 ± 0.61	−0.132	0.896
	<45	24	1.14 ± 0.43		
Tumor size	>2 cm	37	1.29 ± 0.59	3.803	<0.001
	<2 cm	23	0.85 ± 0.30		
Tumor differentiation	I	44	0.98 ± 0.51	−3.873	<0.001
	II	16	1.53 ± 0.44		
Vascular invasion	Y	40	1.25 ± 0.60	3.158	0.003
	N	20	0.87 ± 0.36		
Nerve invasion	Y	48	1.23 ± 0.53	3.030	0.004
	N	12	0.73 ± 0.39		
Lymph node metastasis	Y	22	1.54 ± 0.40	5.553	<0.001
	N	38	0.88 ± 0.46		
Distant metastasis	Y	6	1.83 ± 0.22	3.655	0.001
	N	54	1.05 ± 0.51		

differentiation. To our knowledge, this is the first study to have demonstrated changes in the expression of *HOXA7* in OSCC. In addition, we demonstrated that *HOXA7* expression was correlated with clinicopathological features in OSCC.

Homeobox (HOX) genes are important transcriptional regulators in normal tissue during development. *HOXA7* expression undergoes cell type- and stage-specific changes during ovarian folliculogenesis (16) and is also thought to be highly correlated with the genesis of ovarian epithelial tumors. Expression of *HOXA7* mRNA is higher in epithelial ovarian cancer than in benign tumors (10), and *HOXA7* antibody in serum can be applied for diagnosis of ovarian epithelial cancer (17). *HOXA7* also

stimulates human hepatocellular carcinoma proliferation through regulation of cyclin E1/CDK2 (18). In addition, *HOXA7* has been reported to regulate the differentiation of promyelocytic leukemia (19). Our study of OSCC has broadened the potential roles of *HOXA7* in development and progression of malignancy.

Here we found that *HOXA7* expression at the mRNA and protein levels was enhanced in squamous cell carcinoma. This result is consistent with previous research that has also indicated high expression of *HOXA7* in ovarian cancer and hematopoietic tumors in comparison with corresponding normal tissues (20,21). Thus, we infer that the *HOXA7* gene can serve as an independent tumor growth factor in several types of cancer. Li et al. (18) have reported that *HOXA7* might stimulate hepatic carcinoma by promoting the expression of cell cycle protein E1/CDK2. In addition, *HOXA7* has been considered an important target for methylation, which initiates tumorigenesis. However, the regulatory mechanisms of *HOXA7* in the development of OSCC require further study.

Although *HOXA7* expression has been reported in the tumorigenesis of several types of cancer, its correlation with clinicopathological features has not been studied previously. Our data suggested that *HOXA7* expression at the mRNA and protein levels was correlated with advanced OSCC stages and disease severity, including features such as poor tumor differentiation, vascular and nerve invasion, and increased lymph node and distant metastasis. In this study, IHC was applied to detect the level of expression of *HOXA7* protein. We analyzed the data in terms of two different parameters: the rate of positive staining and MOD. Although some inconsistent results were found, most of the data were further confirmed by real-time PCR.

Despite advances in the diagnosis and surgical treatment of OSCC, the mortality rate has remained unchanged. A better molecular and clinical staging system for OSCC is needed, and this would allow more specific and individualized therapy. At the molecular level, increased expression of *HOXA7* activates both AKT and the canonical EGFR signaling pathway, resulting in increased cell proliferation and chromosomal instability. Inactivation of tumor suppressors such as p16 and p53, and overexpression of oncogenes such as EGFR, c-myc, and PRAD-1 are also involved in OSCC development (22). In this study, for the first time, we have demonstrated that *HOXA7* is overexpressed in OSCC and that its expression is correlated with disease severity, adding to existing knowledge of the molecular network underlying OSCC tumorigenesis.

In conclusion, our present study has shown that *HOXA7* expression is increased in OSCC relative to normal tissues. Further study is needed to examine the mechanism of *HOXA7*-induced tumorigenesis and the signaling pathway involved. Our study provides valuable information that could aid the early detection, diagnosis and therapy of OSCC.

Acknowledgments

This study was supported by the China-British Joint Molecular Head and Neck Cancer Research Laboratory at the School of Stomatology, Guizhou Medical University and Science and Technology Fund of Guizhou Province (Grant No. Qian Ke He LH Zi[2015]7420)

Conflict of interest

The authors have no conflict of interest to declare.

References

1. Ferlay J, Shin HR, Bray F, Forman D, Mathers C, Parkin DM (2010) Estimates of worldwide burden of cancer in 2008: GLOBOCAN 2008. Int J Cancer 127, 2893-2917.
2. Zhang SK, Zheng R, Chen Q, Zhang S, Sun X, Chen W (2015) Oral cancer incidence and mortality in China, 2011. Chin J Cancer Res 27, 44-51.
3. Xu JL, Xia R, Sun L, Min X, Sun ZH, Liu C et al. (2016) Association of CYP1A1 MspI polymorphism with oral cancer risk in Asian populations: a meta-analysis. Genet Mol Res 15, doi: 10.4238/gmr.15027688.
4. Pereira LH, Reis IM, Reategui EP, Gordon C, Saint-Victor S, Duncan R et al. (2016) Risk stratification system for oral cancer screening. Cancer Prev Res (Phila) 9, 445-455.
5. Peisker A, Raschke GF, Guentsch A, Roshanghias K, Eichmann F, Schultze-Mosgau S (2016) Longterm quality of life after oncologic surgery and microvascular free flap reconstruction in patients with oral squamous cell carcinoma. Med Oral Patol Oral Cir Bucal 21, e420-424.
6. Armat M, Ramezani F, Molavi O, Sabzichi M, Samadi N (2016) Six family of homeobox genes and related mechanisms in tumorigenesis protocols. Tumori 2016, 236-243.
7. Teh MT, Hutchison IL, Costea DE, Neppelberg E, Liavaag PG, Purdie K et al. (2013) Exploiting FOXM1-orchestrated molecular network for early squamous cell carcinoma diagnosis and prognosis. Int J Cancer 132, 2095-2106.
8. Gomes AR, Zhao F, Lam EW (2013) Role and regulation of the forkhead transcription factors FOXO3a and FOXM1 in carcinogenesis and drug resistance. Chin J Cancer 32, 365-370.
9. Zhang Y, Cheng JC, Huang HF, Leung PC (2013) Homeobox A7 stimulates breast cancer cell proliferation by up-regulating estrogen receptor-alpha. Biochem Biophys Res Commun 440, 652-657.
10. Ota T, Gilks CB, Longacre T, Leung PC, Auersperg N (2007) HOXA7 in epithelial ovarian cancer: interrelationships between differentiation and clinical features. Reprod Sci 14,

605-614.
11. Yang YC, Wang SW, Wu IC, Chang CC, Huang YL, Lee OK et al. (2009) A tumorigenic homeobox (HOX) gene expressing human gastric cell line derived from putative gastric stem cell. Eur J Gastroenterol Hepatol 21, 1016-1023.
12. Calvo R, West J, Franklin W, Erickson P, Bemis L, Li E et al. (2000) Altered HOX and WNT7A expression in human lung cancer. Proc Natl Acad Sci USA 97, 12776-12781.
13. Cillo C, Schiavo G, Cantile M, Bihl MP, Sorrentino P, Carafa V et al. (2011) The HOX gene network in hepatocellular carcinoma. Int J Cancer 129, 2577-2587.
14. Zhu G, Li J, He L, Wang X, Hong X (2015) MPTP-induced changes in hippocampal synaptic plasticity and memory are prevented by memantine through the BDNF-TrkB pathway. Br J Pharmacol 172, 2354-2368.
15. Zhu G, Wang Y, Li J, Wang J (2015) Chronic treatment with ginsenoside Rg1 promotes memory and hippocampal long-term potentiation in middle-aged mice. Neuroscience 292, 81-89.
16. Ota T, Choi KB, Gilks CB, Leung PC, Auersperg N (2006) Cell type- and stage-specific changes in HOXA7 protein expression in human ovarian folliculogenesis: possible role of GDF-9. Differentiation 74, 1-10.
17. Naora H, Montz FJ, Chai CY, Roden RB (2001) Aberrant expression of homeobox gene HOXA7 is associated with müllerian-like differentiation of epithelial ovarian tumors and the generation of a specific autologous antibody response. Proc Natl Acad Sci USA 98, 15209-15214.
18. Li Y, Yang XH, Fang SJ, Qin CF, Sun RL, Liu ZY et al. (2015) HOXA7 stimulates human hepatocellular carcinoma proliferation through cyclin E1/CDK2. Oncol Rep 33, 990-996.
19. Jo S, Lee H, Kim S, Hwang EM, Park JY, Kang SS et al. (2011) Inhibition of PCGF2 enhances granulocytic differentiation of acute promyelocytic leukemia cell line HL-60 via induction of HOXA7. Biochem Biophys Res Commun 416, 86-91.
20. Afonja O, Smith JE Jr, Cheng DM, Goldenberg AS, Amorosi E, Shimamoto T et al. (2000) MEIS1 and HOXA7 genes in human acute myeloid leukemia. Leuk Res 24, 849-855.
21. Pando SM, Taylor HS (2002) Homeobox gene expression in ovarian cancer. Cancer Treat Res 107, 231-245.
22. Scully C, Field JK, Tanzawa H (2000) Genetic aberrations in oral or head and neck squamous cell carcinoma (SCCHN): 1. Carcinogen metabolism, DNA repair and cell cycle control. Oral Oncol 36, 256-263.